



РАДИОФИЗИКА, ЭЛЕКТРОНИКА, АКУСТИКА

Известия Саратовского университета. Новая серия. Серия: Физика. 2022. Т. 22, вып. 4. С. 288–309
Izvestiya of Saratov University. Physics, 2022, vol. 22, iss. 4, pp. 288–309
<https://fizika.sgu.ru> <https://doi.org/0.18500/1817-3020-2022-22-4-288-309>, EDN: GLCHRL

Article

Modeling battery systems – problems of nonlinearity, efficiency, aging, coupling, and network setup

V. Anishchenko¹, W. Ebeling², E.-C. Hass³, P. Plath⁴, L. Schimansky-Geier², G. Strelkova¹✉

¹Saratov State University, 83 Astrakhanskaya St., Saratov 410012, Russia

²Humboldt University, Unter den Linden 6, 10117 Berlin, Germany

³University of Bremen, Bibliothekstraße NW 2, 28359 Bremen, Germany

⁴Fritz-Haber-Institut der Max-Planck-Gesellschaft, Faradayweg 4–6, 14195 Berlin, Germany

Werner Ebeling, ebeling@physik.hu-berlin.de, <https://orcid.org/0000-0003-0740-3016>

Ernst-Christoph Hass, echass@uni-bremen.de, <https://orcid.org/0000-0001-6968-455X>

Peter Plath, peter-plath@t-online.de, <https://orcid.org/0000-0002-1914-8318>

Galina Strelkova, strelkovagi@sgu.ru, <https://orcid.org/0000-0002-8667-2742>

Abstract. We discuss several problems of batteries and fuel cells from the point of view of nonlinear dynamics and review some earlier work on modeling this class of systems as well as new developments. We consider batteries and fuel cells as active nonlinear electrochemical circuits with properties depending on many factors as load, age, load history etc. We show that most satisfactory battery regimes are reached by coupling of an odd number of circuits in opposite phases. Specific points of discussion are types of dynamic regimes and the efficiency of the conversion of chemical into electrical energy in dependence on the work load, the life cycles of batteries, including installation, work under load, aging and decay. Further we discuss specific properties of managing battery networks, in particular the cycle of replacing of old batteries by fresh ones including the optimization of this cycle. The last part of this work is merely a list of open tasks to be elaborated.

Keywords: battery, load, aging, battery networks, nonlinearity, efficiency

Acknowledgements: The authors thank U. Erdmann, R. Feistel, B. Lindner, P. Romanczuk and F. Schweitzer for basic common work about active dynamical systems and E. Hildebrandt as well as I. Sokolov for discussions about fractional dynamical models and references.

For citation: Anishchenko V., Ebeling W., Hass E.-C., Plath P., Schimansky-Geier L., Strelkova G. Modeling battery systems – problems of nonlinearity, efficiency, aging, coupling, and network setup. *Izvestiya of Saratov University. Physics*, 2022, vol. 22, iss. 4, pp. 288–309. <https://doi.org/0.18500/1817-3020-2022-22-4-288-309>, EDN: GLCHRL

This is an open access article distributed under the terms of Creative Commons Attribution 4.0 International License (CC0-BY 4.0)

Научная статья

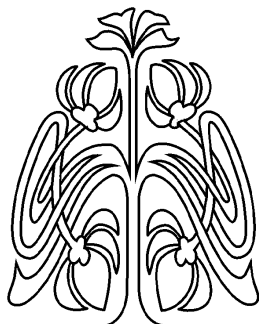
УДК 621.354.36

Моделирование батарейных систем – проблемы нелинейности, эффективности, старения, связи и устройства сети

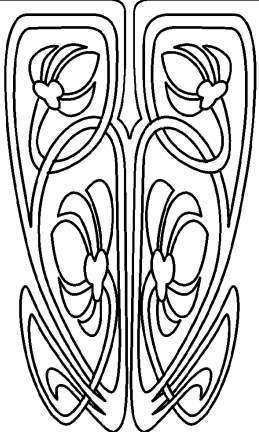
В. Анищенко¹, В. Эбелинг², Э.-К. Хасс³, П. Плат⁴, Л. Шиманский-Гайер², Г. Стрелкова¹✉

¹Саратовский национальный исследовательский государственный университет имени Н. Г. Чернышевского, Россия, 410012, г. Саратов, ул. Астраханская, д. 83

²Гумбольдтский университет, Унтер ден Линден 6, 10117 Берлин, ФРГ



НАУЧНЫЙ
ОТДЕЛ





³Университет г. Бремена, Библиотекштрассе 2, 28359 Бремен, ФРГ

⁴Институт Фрица-Хабера Общества Макса Планка, Фарадейверг 4–6, 14195 Берлин, ФРГ

Эбелинг Вернер, доктор теоретической физики (Dr. Habil.), профессор, Почетный профессор СГУ имени Н. Г. Чернышевского, ebeling@physik.hu-berlin.de, <https://orcid.org/0000-0003-0740-3016>

Хасс Эрнст-Кристоф, доктор естественных наук (PhD), научный сотрудник, echass@uni-bremen.de, <https://orcid.org/0000-0001-6968-455X>

Плат Питер, доктор теоретической физики (Dr. Habil.), профессор, Почетный профессор Бременского университета, peter-plath@t-online.de, <https://orcid.org/0000-0002-1914-8318>

Стрелкова Галина, доктор физико-математических наук, доцент, заведующий кафедрой радиофизики и нелинейной динамики, strelkovagi@sgu.ru, <https://orcid.org/0000-0002-8667-2742>

Аннотация. В настоящей статье обсуждаются некоторые проблемы батарейных систем и топливных элементов с точки зрения нелинейной динамики, и приводится обзор ряда ранних работ по моделированию этого класса систем, а также новые разработки. Батареи и топливные элементы рассматриваются как активные нелинейные электрохимические цепи, свойства которых зависят от многих факторов, таких как нагрузка, старение, история нагрузки и т. д. Показывается, что наиболее удовлетворительные режимы работы батарей достигаются путем соединения нечетного числа цепей в противоположных фазах. Особыми моментами обсуждения являются виды динамических режимов и эффективность преобразования химической энергии в электрическую в зависимости от рабочей нагрузки, жизненных циклов батарей, включая установку, работу под нагрузкой, старение и распад. Далее в статье обсуждаются особенности управления батарейными сетями, в частности, цикл замены старых батарей на новые, включая оптимизацию этого цикла. В заключительной части данной работы приводится список открытых задач и проблем, которые необходимо проработать.

Ключевые слова: батарея, нагрузка, старение, батарейные сети, нелинейность, эффективность

Благодарности: Авторы благодарят У. Эрдманна, Р. Фейстеля, Б. Линднера, П. Романчука и Ф. Швейцера за основную совместную работу по активным динамическим системам и Э. Хильдебрандта, а также И. Соколова за обсуждение дробных динамических моделей и предоставление соответствующих ссылок.

Для цитирования: Анищенко В., Эбелинг В., Хасс Э.-К., Плат П., Шиманский-Гайер Л., Стрелкова Г. Моделирование батарейных систем – проблемы нелинейности, эффективности, старения, связи и устройства сети // Известия Саратовского университета. Новая серия. Серия: Физика. 2022. Т. 22, вып. 4. С. 288–309. <https://doi.org/0.18500/1817-3020-2022-22-4-288-309>, EDN: GLCHRL

Статья опубликована на условиях лицензии Creative Commons Attribution 4.0 International (CC-BY 4.0)

Introduction

The working paper written at the Mini-Workshop “Nonlinear Battery Models” (September 2, 2019), organized by P. Plath at time of the International Conference “Dynamic Days Europe” (September, 2019, Rostock, Germany). In the meantime, two of the present authors (Vadim Anishchenko and Lutz Schimansky-Geier) passed away, so this working paper is to be considered as a historical document, witnessing a long-standing collaboration.

Electrochemical batteries and fuel cells are nowadays the key technologies of our time which more and more replace classical technologies based on combustion. In particular Lithium-ion batteries have become the most common rechargeable batteries for consumer electronics and automotive applications due to their high energy densities, decent power density, relatively high cell voltages, and low weight-to-volume ratios. The same actuality has fuel cells which are perspective also for motor industry etc. There are also some new developments in the field exploring new devices as e.g. the vanadium redox-flow batteries, sodium batteries and ammonia-fed fuel cells. For improving battery and fuel cell performance have intensified the need for mathematical modeling. Modeling and simulations allow for the analysis of an almost un-

limited number of design parameters and operating conditions at a relatively small cost. Experimental tests are used to provide the necessary validation of the models. For a battery manufacturer, models and simulations help to improve the materials and the design of battery systems. It has been shown that concepts of synergetics may be helpful for battery – determination and forecast of the dynamical behavior including aging [1]. There exist many works modeling batteries as nonlinear circuits by means of differential equation calculus [2–8], including problems of efficiency [6, 9]. In order to demonstrate a new development in chemical storage, we also include a discussion of a new type of batteries, the vanadium redox-flow batteries [8, 10, 11]. The vanadium redox battery, also known as the vanadium flow battery, is a type of rechargeable flow battery that employs vanadium ions in different oxidation states to store chemical potential energy [8, 10, 11]. In many respect, batteries may be considered to be very specific in some respects in comparison to standard nonlinear circuits. Specific properties can be related to the fact that batteries are dynamical systems with life cycles like living creatures, including birth, growing, working under load, aging and taking out of the system. These specific properties are responsible for rather spe-



cial elements in our nonlinear models which remind even some models of biosystems [6].

1. Experimental monitoring of the aging process of batteries

1.1. Internal measurements at different locations within the battery

We assume that the aging of a battery is not considered as abrasion or poisoning of the battery, but it is caused by the process of dynamics of charging and discharging. We further suppose that this applies in principle to any type of battery. We have carried out our investigations using lead-acid batteries as examples, which are used for instance in hundreds of millions as starter batteries, where understanding how they work is of great relevance even today. These tests and the data evaluation were performed by us according to our ideas and specifications using software developed by us. The company VB Autobatterie GmbH (formerly Varta) gratefully provided us with its test utility and a workplace to conduct our measurements under industrial conditions. In an additional internal study in cooperation with Dt. Accumotive GmbH & Co. KG, which was also carried out according to our specifications and evaluated by us, we were able to

show that the principle results obtained for lead-acid batteries can also be applied to Li-ion batteries.

In order to perform internal measurements within a lead-acid battery, the measuring electrodes must be durable, unbreakable and mechanically stable and must not be chemically altered by the actual process. It follows that the measuring electrodes themselves must be made of lead. In addition, it must be ensured that the packing of the battery stacks and their geometry are not changed in the process. Figure 1 shows the experimental test arrangement for two lead-acid batteries, each with 10 measuring probes. A more detailed description of the measurement system can be found in reference [1].

Furthermore, the selection of the battery cell stacks, and the arrangement of the probes in relation to the poles plays a major role. Both the temperature development and the current flow must be taken into account. For starter batteries with 6 stacks each, we have therefore selected the middle cell as shown in Fig. 2 (left panel). Another problem is that in a lead-acid battery, the density of the acid and the acidity is a function of the charging and discharging process. In other words, locally different electrochemical processes change the degree of

Two batteries with 10 measuring probes each

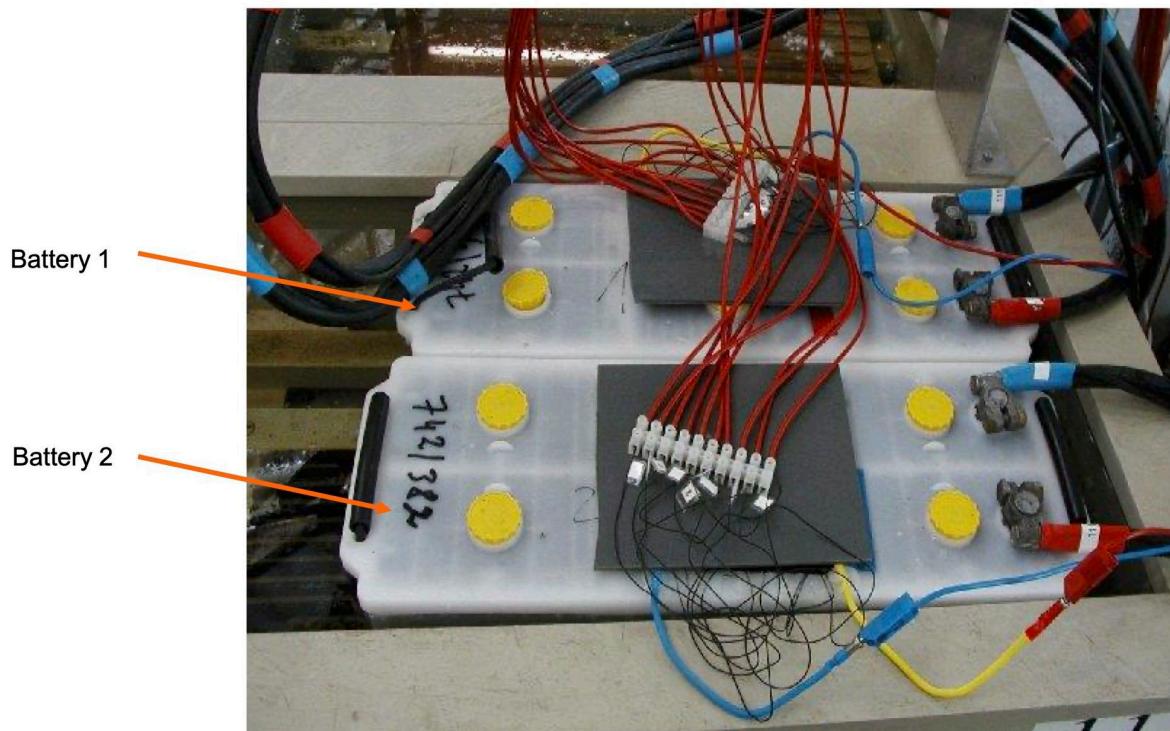


Fig. 1. View of two lead-acid batteries in the test laboratory at VB Autobatterie GmbH



acidity in the different layers of the battery. Thus, if one wants to record the spatial and temporal variation of dynamics in a battery, one must provide measuring probes both at different heights of a cell and at different lateral positions. An arrangement of measuring probes in a cell resulting from these considerations is shown in Fig. 2 (right panel).

Discharging and recharging of the battery was done by the test program AK 3.4 of the company VB Autobatterie GmbH and the recording of the voltage responses at the individual positions by our own software developed for this purpose. Figure 3 shows exemplarily the rectangular driver pulse due to the

discharge and charge currents (red) as well as the voltage curve of the battery's response (black) for 5 cycles within about 6 hours. The response behavior of the battery, with which it reacts to the perturbation, does not follow the rectangular pulse in a simple way, but corresponds to the intrinsic times of the system and makes it possible to determine the age of the battery. However, we cannot exclude the possibility that the battery may also experience autonomous oscillations.

Figure 4 demonstrates the aging of a battery by means of the voltage curve of the total battery voltage in comparison to the simultaneous voltage curve

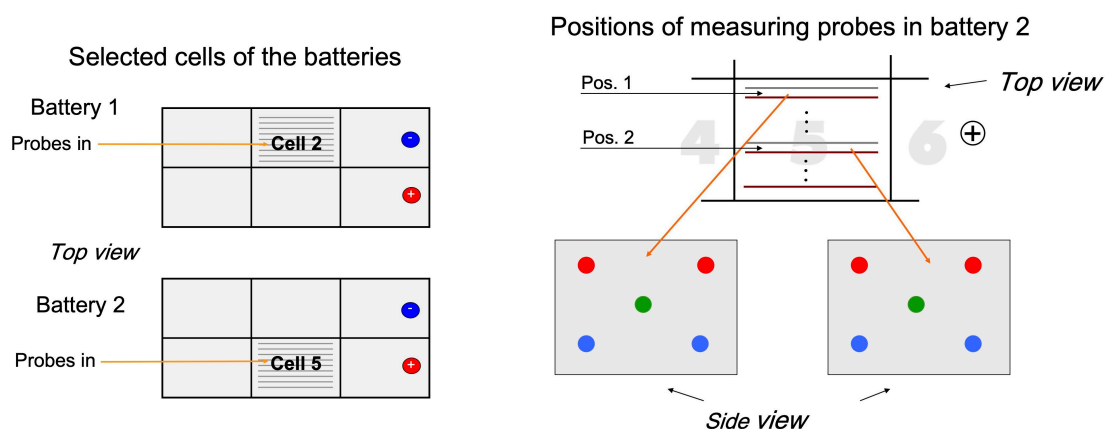


Fig. 2. Left panel: Selected cells where the probes are placed within two batteries. Right panel: Positions of measuring probes in cell 5 of battery 2. In two different heights, 5 measuring electrodes each are arranged according to the side view shown in the Figure

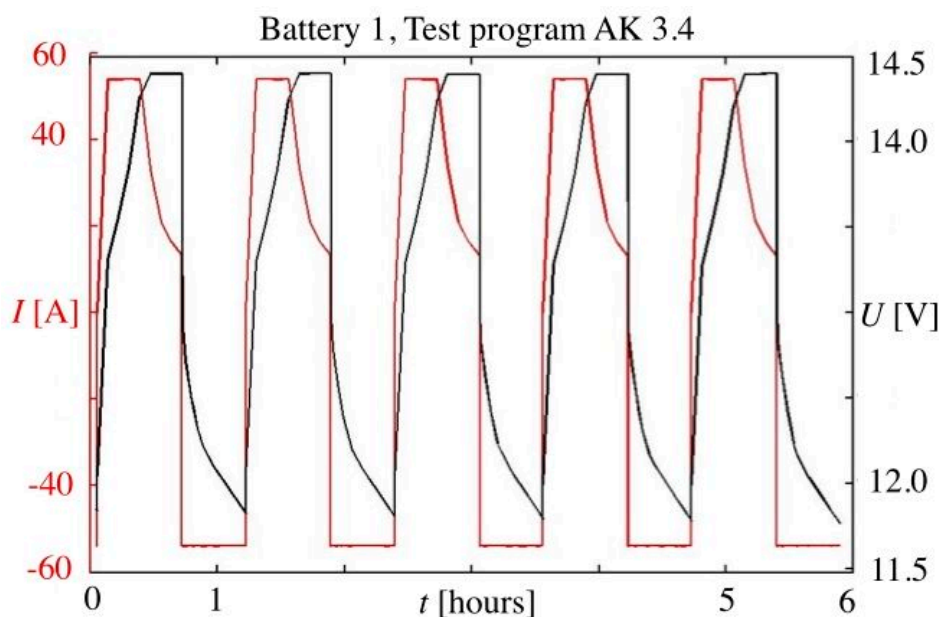


Fig. 3. Rectangular driver pulse due to the discharge and charge currents (red) and the voltage curve of the battery's response (black) for 5 cycles within about 6 hours. The industrial test program AK 3.4 of VB Autobatterie GmbH was operated in such a way that the maximum voltage was limited to 14.4 V during charging in order to prevent overcharging of the accumulator (color online)

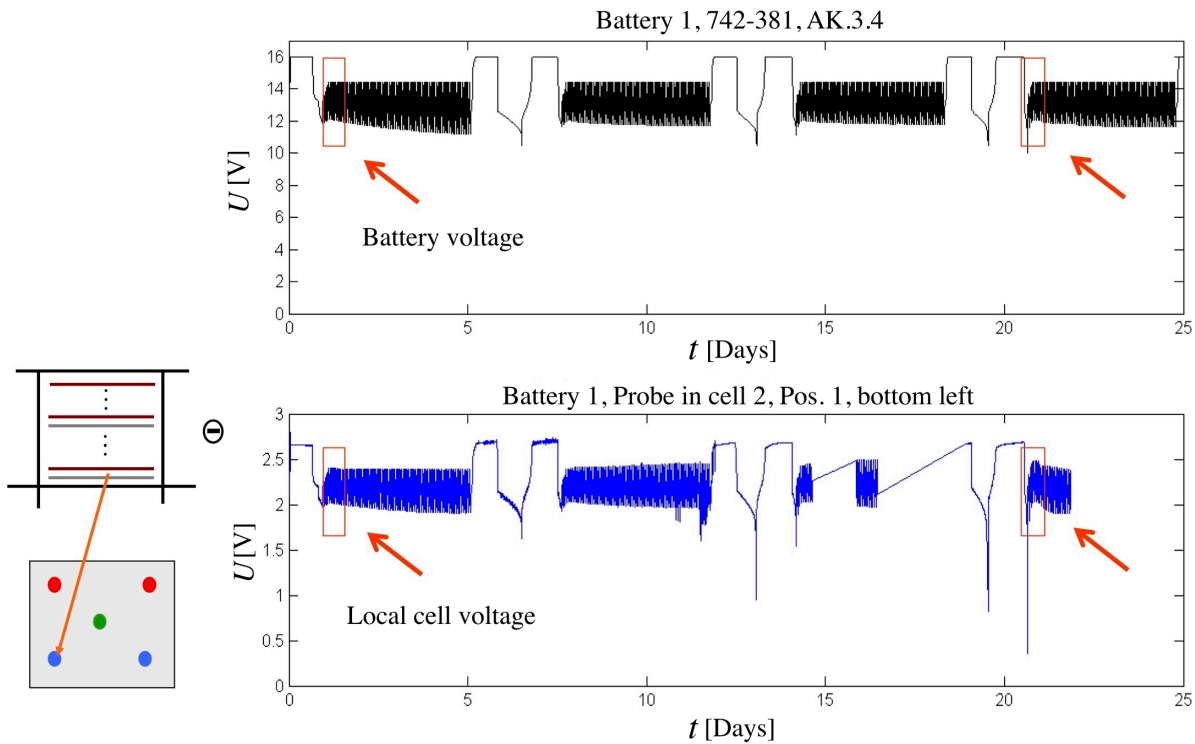


Fig. 4. Aging of a battery demonstrated by the voltage curve of the total battery voltage compared to that of a single measuring probe near a corner at the bottom of the cell (color online)

of a single measuring electrode, which is located near a corner at the bottom of the cell at high acid concentrations. In these experiments, aging was generated by longer periods of alternating charge and discharge cycles, as is common in industrial technology. One week of these measurement cycles corresponds approximately to the aging of a battery within one year in normal operation. The performance of the battery, i.e. its State of Health (SoH), after such a one-week treatment or an annual aging period was tested by extreme load experiments.

An impression of the aging process of a battery can already be obtained by comparing the total battery voltage during the discharging and charging processes in its new and in its aged state. These discharging and charging processes are by no means cyclic ones in the form of a limit cycle. Figure 5 illustrates this in a compressed 3-dimensional phase space representation of the delay attractors of the battery voltage at the beginning of the test as well as after approx. 3 weeks corresponding to about 3 years of treatment of the battery.

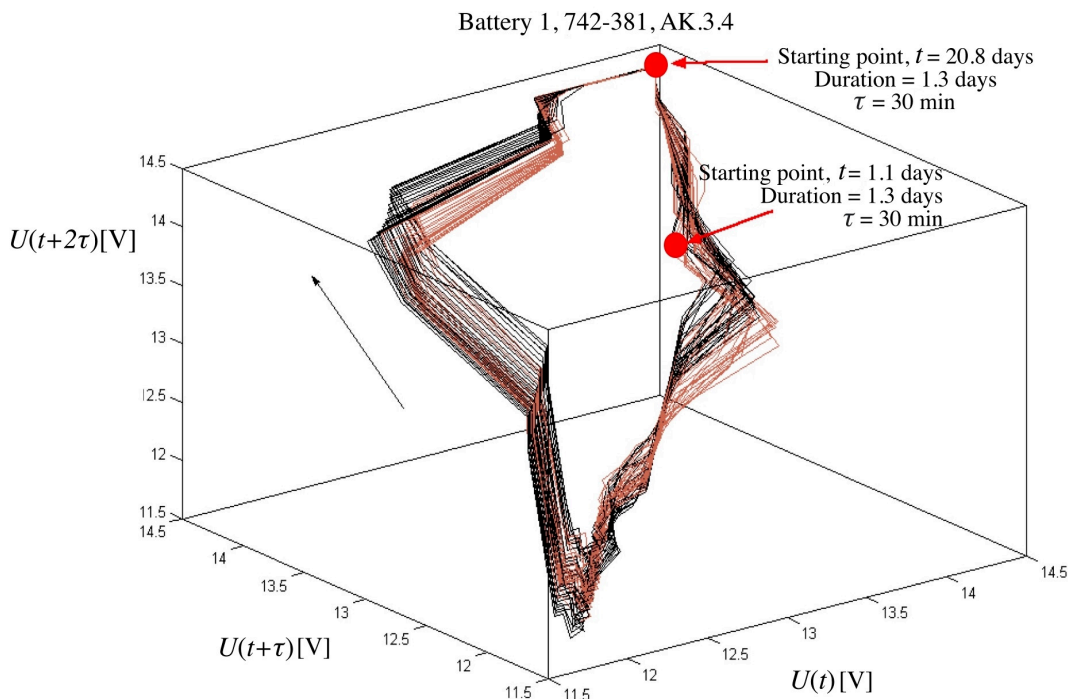
More detailed information than from battery voltage is obtained from spatio-temporal voltage measurements of individual probes. Figure 6 shows the time series of local potentials corresponding to

4 probes in 4 different lower positions within the stack at strong acid concentration, measured against the positive electrode over a period of about half a week. It can be clearly seen that the voltage curves at the different positions lead to different time series.

1.2. Empirical evidence for aging processes

The aging of a battery is particularly evident if one compares the delay attractors of voltages of a single probe with those of total battery voltages. In contrast to Fig. 5, Fig. 7 shows the aging using the example of the delay attractors of a centered measuring probe in front stack position in cell 2. Already after 3 weeks corresponding to 3 years of battery aging, the attractor (yellow) deviates significantly from the healthy state (green) and grows excessively shortly before the end of battery lifetime (red).

The different time series of local potentials (see Fig. 6) and their attractors make it clear that there is no uniform aging process within the battery, but that different locations between the electrode plates behave in different ways, even within a layer of the same acid concentration. This also means that the system acts chemically differently at different loca-



Measured values from VB Autobatterie GmbH

Fig. 5. 3-dimensional phase space representation of the delay attractors of the battery voltage at the beginning of the test and after approx. 3 weeks of treatment of the battery. In each case, the duration of the test period amounts to 1.3 days and the delay value τ is 30 minutes (color online)

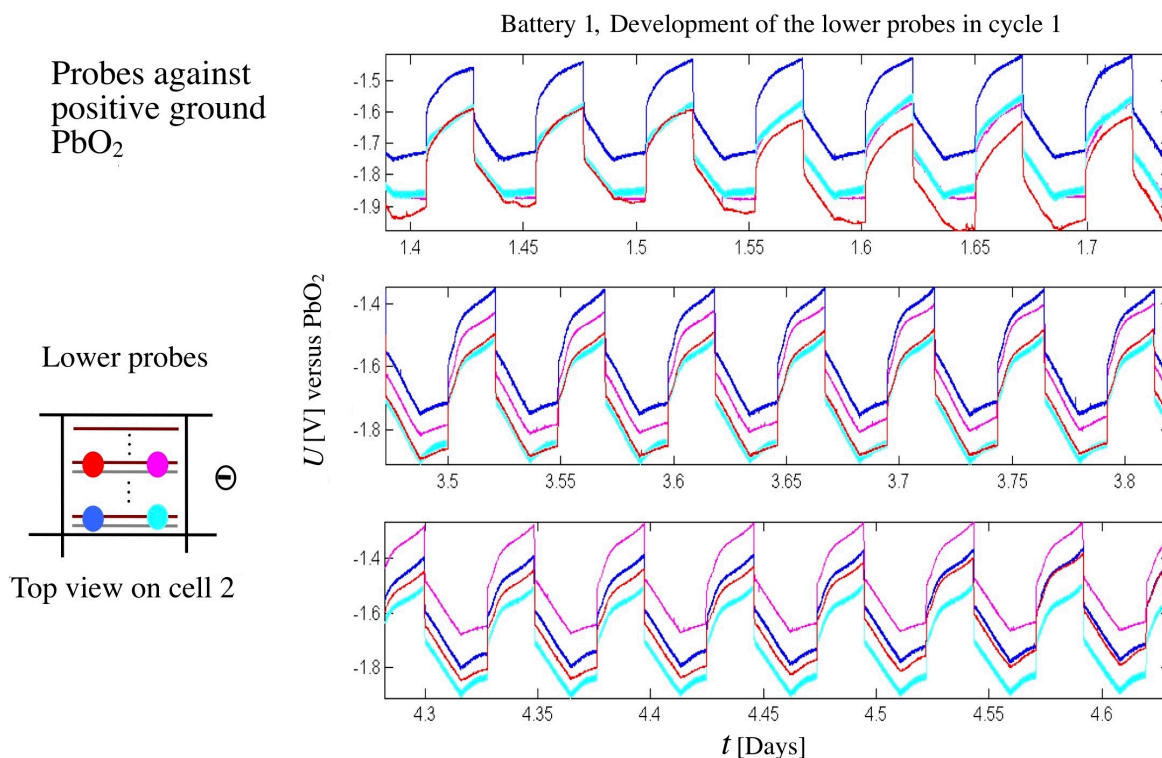


Fig. 6. Time series of the local (half-) potentials of four probes in lower positions as indicated, measured versus the positive mass PbO_2 . The 3 diagrams, arranged under each other, correspond to three different time intervals of measuring cycles (30 min discharging, 40 min charging, both with about 53.9 A) (color online)

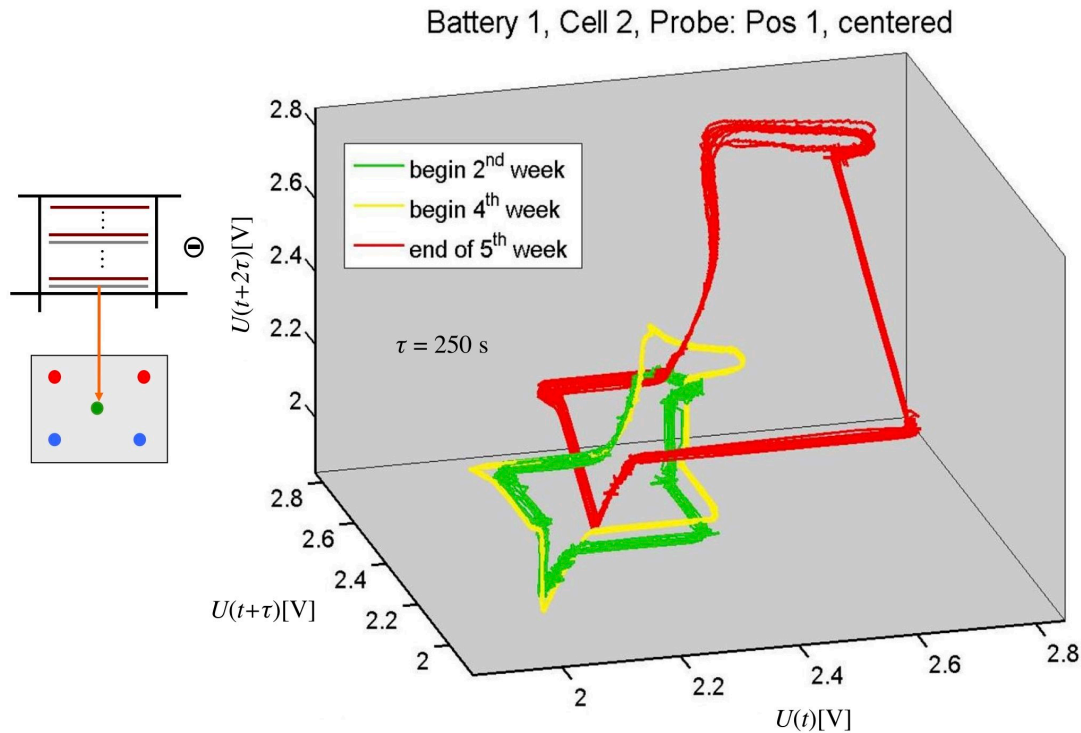


Fig. 7. 3-dimensional delay attractors of local potentials measured by a centered measuring probe located in front stack position in cell 2. The delay time of each attractor is $\tau = 150$ s. The attractors were obtained at the beginning of the 2nd and 4th week as well as at the end of the 5th week for approximately 8 discharge and charge cycles each at approximately 53.9 A (color online)

tions in its development over time, i.e. in the way a position ages, its chemical behavior also changes. Therefore, it cannot be assumed that the electrochemical processes taking place at the electrodes of the battery are synchronous and uniform; instead, due to the non-synchronous reaction behavior between the lead plates, spatio-temporal patterns are formed that are characteristic for the aging state of the battery. From these patterns and their temporal development, the aging state of a battery can be determined using the methods of synergetics.

Battery aging is thus a highly complex process that is only incompletely described by the existing methods as we have shown for the lead-acid battery. Of course, the forms of aging, and thus the attractors of aging, are different for other types of batteries, such as the Li-ion battery, due to their different chemistry, and each battery type requires a different experimental setup to take this into account. This reveals a weakness in current battery research, which is focused mainly on the investigation of numerous electrochemical systems to optimize the desired battery performance. But all batteries are aging. A general possibility to detect the aging state of a battery by short-time measurements at the battery

poles with periodic excitations can also be found in [1].

2. Modeling electrochemical batteries and fuel cells as active circuits

2.1. Basic schema of active currents driven by chemical energy

We consider electrochemical batteries and fuel cells as active nonlinear circuits with special properties in difference to other active circuits which were studied in much detail [2, 3]. Standard models of batteries and fuel cells were described in [4]. Our model is based on the analogy between active electrical circuits and active particles [6, 9]. Specific points of the discussion here are the facts that in particular the most popular batteries, the Lithium cells batteries are dynamical systems which much in common with biological creatures. For example, they have life cycles like biological species, including birth, growing, working under load, aging and decaying (taking out of the system after collapse of the function). Conversion of energy by means of irreversible processes and dissipative structures is not new; various technical and biological systems function this way. If we restrict ourselves to systems



with chemical energy input, we may distinguish between converters to, e.g., mechanical, electrical or radiation energy. Here we briefly discuss typical efficiencies of some traditional “engines” of this particular type. Mechanical work is obtained from the chemical energy of fuels by combustion of raw materials such as wood, coal, oil or gas. The engines are kinds of self-sustained nonlinear oscillators such as steam engines, combustion motors or jet plane turbines. As far as the fuel is burned and the resulting heat is used as an energy pump of the nonlinear oscillator, the efficiency of such machines cannot exceed that of the thermodynamic Carnot cycle, as a consequence of the 2nd law. Fuel cells are devices that convert chemical energy to electrical energy without the intermediate stage of producing and consuming heat. Typical efficiencies of fuel cells range from 20 percent to 70 percent [7]. In difference to fuel cells, the mechanism of batteries is based on a closed cycle. First the electrical energy is stored into chemical energy inside the cell and in the second half of the cycle this chemical energy is converted into electrical energy.

Similar to the dissipative structures of steam engines or gas turbines, a fuel cell will “starve” at subcritical values of the energy pumping rate. In this article, a theoretical model will be described for alternative, self-organized processes that may act like a fuel cell. As already said, a fuel cell is a device that converts the chemical energy from a fuel like hydrogen gas into electricity through a chemical reaction of positively charged hydrogen ions with oxygen or another oxidizing agent. This process requires a continuous source of fuel such as hydrogen and oxygen to sustain the chemical reaction of the fuel with the oxidizing agent. Fuel cells can produce electricity, by exploiting the input of chemical energy [12]. For a fuel cell to produce electricity, it must be continually supplied with fuel and oxidant. The details of this mechanism can be quite complicated. We will study here only a simplified schema which we call “*active circuit*”. The model should reflect at least in a rudimentary form the following observed physical properties of fuel cells: When a fuel cell is operated with high output, i.e. high current, its demand for reactants is large. If the reactants are not supplied to the fuel cell quickly enough, the device will starve. The work of fuel cells is based on electrochemical reactions, connected with the fuel, e.g. hydrogen, the oxidizer and charges. Once the reactants are delivered to electrodes, they must undergo electrochemical reactions. The current generated by the

fuel cell is directly related to how fast the electrochemical reactions proceed. Fast electrochemical reactions result in a high current output from the fuel cell. Slow reaction results in a low current output. As a promising new direction of development, we mention the ammonium-based fuel cells [12]. Ionic conduction happens through the electrolyte and electron conduction through the external circuit. The electrochemical reactions occurring in step 2 either produce or consume ions and electrons. Ions produced at one electrode must be consumed at the other electrode. The same holds for electrons. To maintain charge balance, these ions and electrons must therefore be transported from the locations where they are generated to the locations where they are consumed. For electrons this transport process is rather easy. As long as an electrically conductive path exists, the electrons will be able to flow from one electrode to the other.

In detail all these processes are extremely complex and there exists a big variety of models [13–15]. We are studying here only macro models for the functioning of batteries and fuel cells, which operate in a space of a few time-dependent variables as charge, current and energy content. Figure 8 shows several schemes of macro models (Ersatzschaltbild) used for modeling batteries, as used e.g. by Eckert [14] (left panel) and by Wang et al. [15] (right panel).

The highly simplified schema which we use to model the quite complex processes in real systems is the following. The active particles in our schema are the charges. For simplicity, we study only two variables for the characterization of the electric state, the charge of the capacitor Q and the current $I(t)$ in the circuit. The charge is a variable which may increase or decrease and is therefore a dynamic quantity $Q(t)$. The charge may increase or decrease following the consumption of fuel and is connected with a current $I(t)$. The third relevant dynamical variable is the energy contained in the chemical reactor $E(t)$ which is driving the electric current I in the circuit.

This way we have to define at least 3 differential equations that specify the dynamics of the fuel cell within our model which we expect to work with modifications also for batteries

$$\begin{aligned} \frac{dQ(t)}{dt} &= I(t), \\ \frac{dI(t)}{dt} &= F_2(I(t), E(t), Q(t)), \\ \frac{dE(t)}{dt} &= F_3(E(t), I(t)). \end{aligned} \quad (1)$$

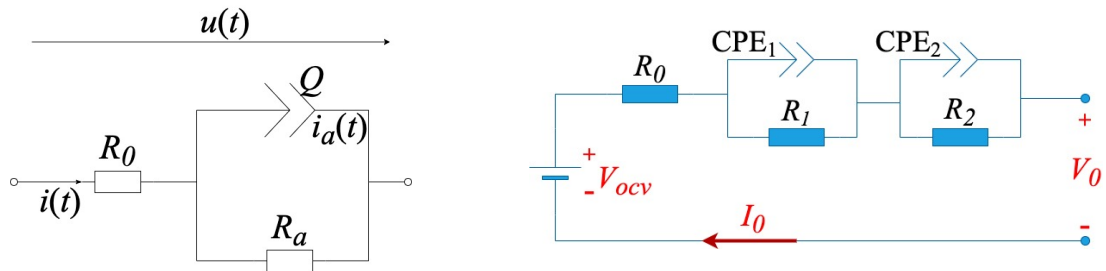


Fig. 8. Schema of the simple battery model used by Eckert [14] (left panel) in comparison to the more advanced model proposed by Wang et al. [15] (right panel) (color online)

The two functions F_2, F_3 modeling the energy flow from the chemical reactor/capacitor to the current in the circuit have still to be determined in a way that the properties of the fuel cell which we described above are reflected at least in a qualitative way. This will be done in the next section.

There are several properties which are relevant for an efficient regime of fuel cells, which however are not principal ingredients and will not be modeled here. For example, the efficient delivery of reactants is more effectively accomplished by using flow field plates in combination with porous electrode structures. Flow field plates contain many fine channels or grooves to carry the gas flow and distribute it over the surface of the fuel cell. The shape, size, and pattern of flow channels can significantly affect the performance of the fuel cell. Obviously, high current output is desirable. Therefore, catalysts are generally used to increase the speed and efficiency of the electrochemical reactions. Fuel cell performance critically depends on choosing the right catalyst and carefully designing the reaction zones. Specific points of discussion are the facts that batteries and fuel cells are dynamical systems having life cycles like living creatures, including birth, growing, working under load, aging, failure and taking out of the system.

2.2. Storing electrical energy in electrochemical systems – redoxflow batteries

We concentrate in this work on the half-cycle connected with the conversion of chemical into electrical energy. The other half-cycle, connected with storing chemical energy may be modeled principally in the same way as the reverse process. However, since several details of this inverse model, mainly connected with stability, are still open, we discuss the storage of electrical energy electrochemically only in general terms. Storing electrical energy electrochemically is a quite old invention of physicists and chemists, recently due to urgent

needs of storage, we see many new developments and interesting inventions. We discuss here the principle of chemical storage on the case of a quite recent and at the same time transparent method, the vanadium redox-flow battery. The vanadium redox battery employs vanadium ions in different oxidation states to store chemical potential energy [8]. The vanadium redox battery exploits the ability of vanadium to exist in solution in four different oxidation states, and uses this property to make a battery that has just one electro-active element instead of two. In the general schema, we have two liquids, one contains two areas of V^{4+} -ions separated by a semipermeable membrane from the other liquid with V^{2+} and V^{3+} . In the work cycle of the battery generating energy (discharging) we observe that at the positive electrode V^{5+} is reduced to V^{4+} . At the same time, we see at the negative electrode that V^{2+} is oxidized to V^{3+} . The energy rich liquids are stored by pumping in two extra tanks which define the capacity. The fact that the tanks are, with respect to their size, independent on the size of the cell device, is one of the advantages of the redox-flow battery. For several reasons, including their relative bulkiness, most vanadium batteries are currently used for grid energy storage, i.e., attached to power plants or electrical grids. The possibility of creating a vanadium flow battery was explored already in the 1970s. The first successful demonstration of the all-vanadium redox-flow battery which employed vanadium in a solution of sulfuric acid in each half was by Rychcik and Skyllas-Kazacos in the 1980s [8].

The redox-flow battery based on vanadium electrochemistry is a promising candidate for load leveling and seasonal energy storage in small grids and stand-alone photovoltaic systems. The reversible cell voltage of 1.3 to 1.4 V in the charged state allows the use of inexpensive active and structural materials. Another promising direction is the development of sodium-based batteries [12].



3. Dynamics of nonlinear electrochemical circuits

3.1. Active electrochemical circuits

We model here the processes of conversion of chemical energy into work in batteries and fuel cells by using the analogy to active particles [6,9]. Standard models are described by Newman [4]. We describe here only homogeneous models based on thermodynamic balances and the idea of active circuits. Active circuits are the electrical analog to active mechanical particles [16, 17]. An active circuit is an electrical system consisting of an *RCL*-circuit including elements with “negative resistance” [2]. We assume a dynamics of the following type for a charge $Q(t)$, a current $I(t)$ and a chemical energy $e(t)$

$$\frac{dQ(t)}{dt} = I; \quad \frac{de}{dt} = q_e - ce - deI^2, \quad (2)$$

$$L \frac{dI}{dt} = -RI - \frac{Q}{C} + U_0 + deI, \quad (3)$$

Here, q_e means the chemical energy flow, c is the decay rate and d is the rate of transmission of depot energy to energy of motion, L is the impedance, R is the resistance, C is the capacity, and U_0 is a kind of external load which in the case $U = -a < 0$ is a load to overcome. For example, we may assume that a charge Q is to transfer to a higher level of the electrical potential, i.e. work is to be done. In the case that the energy assumes stationary values, the system may be reduced to the model of a driven electrical oscillator. For modeling a specific battery, we may use the simple schema by Eckert shown in Fig. 8 (left panel). According to Kirchhoffs rule, we find for the big loop

$$U(t) + I_0(t)R_0 + I_a(t)R_a = 0 \quad (4)$$

and accordingly we get for the active loop

$$R \frac{dQ}{dt} + \left[L \frac{d^2Q}{dt^2} + \frac{Q}{C} - d_e e(t) \frac{dQ}{dt} \right] = 0. \quad (5)$$

Here the second term in parenthesis stands for the double arrow in Fig. 8, i.e. a (large) capacity C , a (small) impedance L , which we add for generality, and the most essential chemical source of energy which follows

$$\frac{de}{dt} = q_e - ce - d_e e \left[\frac{dQ}{dt} \right]^2. \quad (6)$$

The feeding by chemical energy with the flow $q_e > 0$ makes the small circuit an active element. The loss in chemical energy drives the current and charges

the capacitor. The active process of energy conversion of chemical into electrical energy is symbolized graphically in Fig. 8 by a double arrow. The system possesses in the power regime, where I^2 is created and e is used, a stationary state

$$Q_0 = U_0 C; \quad e_0 = \frac{q_e}{R}; \quad I_0^2 = \frac{q_e}{R} - \frac{c_e}{d_e}. \quad (7)$$

Here c_e denotes internal losses (internal resistivity). In some range of parameters, this state is a stable node. In another range we find an unstable node surrounded by a stable limit cycle, so that the system may develop stable oscillations around this state. Running our dynamics reverse in time, e is created and I^2 is used. This would correspond to a charging regime. Formally we may map this regime to the case $q_e < 0$; $d_e < 0$; $c_e < 0$; $U_0 < 0$. Then the stationary state still exists, but is in general less stable. Thus, the present analysis describes mainly the power regime of our model. In order to give an appropriate stable description of the charging regime, we need some modifications, and this case is still to be explored. In the power regime, our system shows beyond a critical value of $dq_c = RC$ sustained oscillations. Numerical solutions for the power regime of our battery system (Eqs. (2) and (3)) are shown in Fig. 9. In the left panel we show above the oscillating voltage in the big circuit and below in the red curve U_{OCV} the so-called Open Circuit Voltage in the small active circuit. Further we demonstrate in the green curve the current in the active circuit and by the blue curve the chemical energy which shows also small fluctuations.

Electrochemical oscillation phenomena were described already in the foregoing Section. In Figs. 4–6 we see oscillations with frequencies around 0.05 days, i.e. around 1 hour. Other examples were for rechargeable batteries observed in [18]. The authors Li et al. speak in the mentioned work about the battery heartbeats and suggest that the heartbeat is due to a process of self-reorganization of the multi-particle phase-separation dynamics. The subtle oscillatory signals serve as an indicator for the fraction of actively phase-separating particles in real time. Here we leave the question of the physico-chemical origin of the battery heartbeat open and restrict ourselves to the question of modeling by an active system.

We investigate now our model system (2) and (3) with respect to oscillations. A special example for an oscillating solution of our full model system (Eqs. (2) and (3)) is shown in Fig. 9a. We see the time dependence of charge, current and chemical energy of the battery for solutions of the full system of

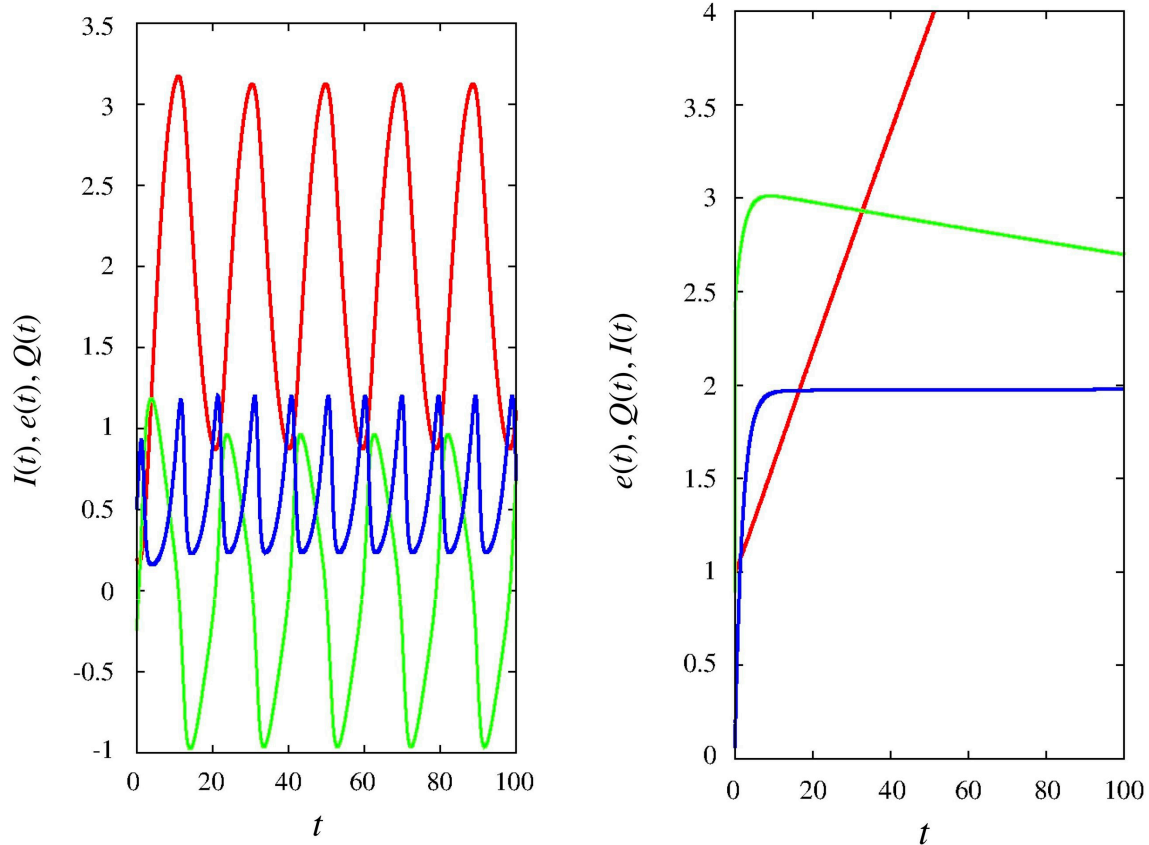


Fig. 9. Left panel: Example of a self-sustained oscillating solution of our model (2), (3) for the charge $Q(t)$ (red), the current $I(t)$ (green) in the active circuit and the chemical energy $e(t)$ (blue). Left panel: Oscillating regime ($q_e = 0.8, c_e = 0.5, d_e = 0.8, U_0 = 1, R_0 = 0.3, L = 1, C = 10$). Right panel: Charging regime with linear increase of the charge $Q(t)$, a maximum and decay of the current and saturation of the chemical depot ($q_e = 1, c_e = 0.5, d_e = 2, U_0 = 1, R_0 = 20, L = 1, C = 50$) (color online)

Eqs. (2) and (3). All quantities oscillate including the chemical energy around the mean value.

Figure 9b shows a completely different situation. We increased here the resistance to the quite high value $R_0 = 20$. The dynamical system is now in an overdamped regime and the oscillations disappear. The chemical depot variable $e(t)$ converges to a constant value and the charge increases in a linear way. The current goes through a maximum and decays then slowly. Possibly this regime may describe the charging regime of a battery. We studied the charging regime also by means of a different model assumption, going to negative parameters and this way to an inverse in time. Simulating several numerical examples with negative parameters we found that this regime describes the conversion of electrical energy into chemical energy only for a finite time, then the regime decays and crashes. The more realistic modeling of the charging regime needs further investigations. More refined models should include positive and negative charges (ions and electrons), so that the current may flow even for zero total charge.

Our model is oversimplified, under more realistic conditions the equivalent circuit for an electrode involves a parallel connection of a capacitance and a Faradaic impedance, the total current thus being composed of a capacitive contribution and a contribution due to the electro-chemical reaction. We concentrated here on modeling the energetic aspect, i.e. the physical fact that the chemical energy generated by the reaction is converted to the energy of the electrical circuit. The reason for neglecting further effects here is not a physical one. Our motivation is to allow a one to one mapping to the solvable mathematics of the model developed by Schweitzer–Ebeling–Tilch (sometimes called SET model). Any additional term would break the possibility for analytical solutions. Our model is in fact nothing more than the extension of the standard circuit equations by a quadratic term in the current which stands for the energy input and makes the circuit active. This additional term is, observing the energy balance, coupled to a simple equation for one reaction. We consider



this as a minimum of relations describing the essence of the energy transfer reaction-current.

The properties of this dynamical system have been studied for the mechanical picture in the works [16,17]. Here we concentrate on the stationary states and questions of energy conversion and efficiency. In the stationary state the chemical energy and the current are given by Eq. (7). As pointed out, this regime is in most cases not stable and dynamically replaced by a stable oscillation around e_0 and I_0 corresponding by a limit cycle. In these cases, the given numbers for e_0 and I_0^2 represent mean values. Then an oscillating current is flowing in the circuit. This current is sustained by the inflow of chemical energy q_e and is dissipated in the resistance R ; further c_e denotes internal losses (internal resistivity). The term $U_d = +deI^2$ denotes the energy transmitted per unit time to the RCL -circuit, i.e. we have a positive energy support. This is an auto-catalytical effect which is essential for the functioning of chemical dissipative structures. Let us still note that in the stationary state the impedance L does not play a big role in the energy balance since the stationary state does not depend on it. A generalization of our model of one circuit coupled to a chemical reservoir leads to the case of two or more equal circles coupled to one chemical reservoir [6]:

$$\frac{dq_1}{dt} = j_1; \quad L \frac{dj_1}{dt} = -Rj_1 - \frac{Q_1}{C} + U_0 + de j_1; \quad (8)$$

$$\frac{dq_2}{dt} = j_2; \quad L \frac{dj_2}{dt} = -Rj_2 - \frac{Q_2}{C} + U_0 + de j_2; \quad (9)$$

$$\frac{de}{dt} = q_e - ce - de(j_1^2 + j_2^2). \quad (10)$$

The two plus one system shows in energetic respect several advantages to the one plus one system since there exists now a class of exact solutions with sinusoidal solutions for $I_1(t); I_2(t)$ in opposite phase and constant in time stable total current energy

$$I_0^2 = j_1^2 + j_2^2 = \frac{q_e}{R} - \frac{c_e}{d} = \text{const}. \quad (11)$$

The corresponding periodic regimes for $j_1(t)$ and $j_2(t)$ in opposite phases show that the electrical energy is periodically exchanged between the two circles. This opens the possibility for more effective regimes of energy conversion. The progress with respect to the task on energy conversion may be compared with progress in motor technology by going from the one cylinder automobile motor to technologies coupling two, four, six or eight cylinder motors. In both cases of one or two circles, the dynamics

of the energy exchange between circuits and chemical processes (e.g. in the fuel cell or at the battery electrodes) is described by balance equations for the electrical energy, which is $E_e \sim (LI^2 + Q^2)/2C$ and the energy of the chemical reactor $e(t)$, the energy inflow q_e and the losses:

$$\frac{dE_{el}}{dt} + \frac{de}{dt} = q_e + U_e I - R(I_1^2 + I_2^2) - c_e e; \quad (12)$$

$$E_{el} = \frac{L}{2} \mathbf{J}^2 + \frac{1}{2C} \mathbf{Q}^2.$$

Here E_{el} is the electrical energy of all units.

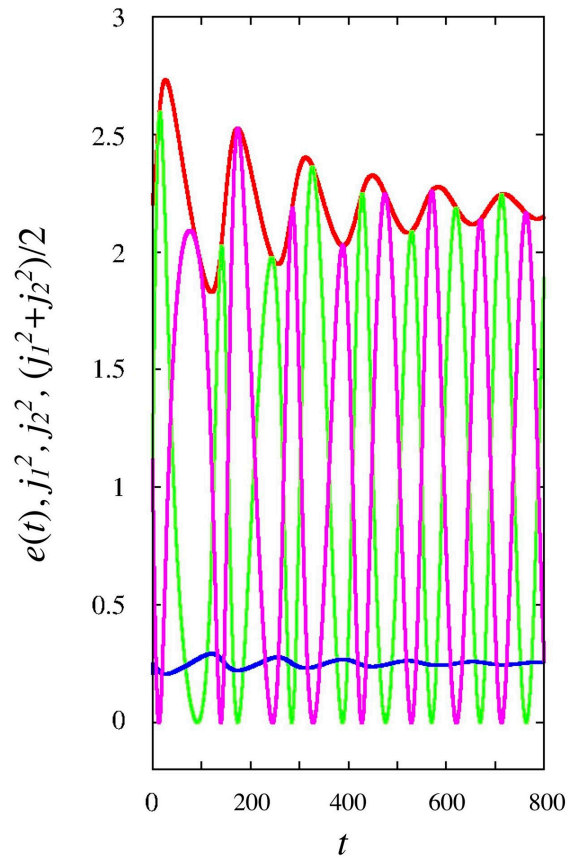


Fig. 10. Example of a solution for the case of two circuits coupled to one electrochemical reservoir. The squared total current $\mathbf{J}^2 = (j_1^2 + j_2^2)$ shown by the red curve above and the content of the chemical reservoir demonstrated by the blue curve below are after a small initial period rather smooth, different from the oscillating current components j_1 and j_2 (green and violet curves, respectively). This corresponds to a more useful regime of the battery system (color online)

In order to demonstrate that our statement about a more useful regime of an even number of battery components, we show examples of a solution for the 1 + 4-dimensional system, i.e. the case of two circuits coupled to one electrochemical reservoir (see Fig. 10). The electrical energy provided by the total



current which is proportional to $(j_1^2 + j_2^2)/2$ represented by the red curve above and the content of the chemical reservoir represented by the blue curve below show after a small initial period a rather smooth regime. This is due to the fact that the individual currents, which still strongly fluctuate, are in counter-phase and give therefore in total a smooth current flow. This corresponds to a more useful regime of the battery system as we observed in case of one circuit. This again reminds us of the analogy to the big progress that the motor industry achieved by coupling an even number of motors operating in counter-phase. Our model for the dynamics of energy conversion in a fuel cell is closely related to some previous work on individual driven particles and driven swarms of active Brownian particles.

3.2. The analogy to active particles, molecular motors and animal motion

This model considers mechanical motion driven by coupling to energy depots, feeded e.g. by the food of animals. The relation to our model of “active circuits” to the widely used biophysical model of active Brownian motion is based on the analogy between mechanical and electrical systems by using the “dictionary”:

mechanical coordinate q	– electrical charge Q ,
velocity $v = \dot{q}$	– current I ,
kinetic energy $k = mv^2/2$	– current energy $\sim I^2$,
mechanical mass m	– impedance L ,
oscillator constant κ	– reciprocal capacity $1/C$,
friction $\rho = m\gamma_0$	– resistance R ,
driving force F_d	– electromotoric force U_d .

In several earlier papers, we studied the dynamic of active mechanical systems with a mass m , located at coordinate $q(t)$ moving with velocity $v(t)$ where $v = \dot{q}$, which is accelerated at the cost of the chemical depot energy e and may perform work against a load:

$$m\dot{v} + \rho_0 v = \mathbf{F}_0 + de\mathbf{v}, \quad \mathbf{F}_0 = -a, \quad a < 0. \quad (13)$$

Here $\mathbf{F}_0 < 0$ is an external force, a load, and for the driving force on cost of a depot energy, we assumed $\mathbf{F}_d = de\mathbf{v}$. This driving force is proportional to the energy depot of chemical nature e , $\rho = m\gamma_0$ a friction constant, and κ some elastic constant, which in most cases is put to zero here.

Within the original SET model, we assumed for the depot energy $e(t)$ the simple dynamics

[6, 19–21]:

$$\dot{e} = q_c - ce - d\mathbf{v}^2 e. \quad (14)$$

The three constants q_c , which is the input rate of depot energy, c , the decay rate and d , the rate of transmission of depot energy to energy of motion, determine the functioning of the motor mechanism. We considered e as a kind of chemical energy as e.g. ATP stored in the depot. The physical meaning is that we have a permanent inflow of energy, which is constant $q_c = \text{const}$, and flows with rate $d\mathbf{v}^2(t)e(t)$ to the mechanical degree of freedom [22, 23]. Note that previously we mainly used units leading to $m = 1$. For $q_0 > \rho_0 c/d$ there exists a stationary point in the positive cone of the energies which corresponds to two stationary points in the phase space. This corresponds for the force-free case to two velocities for the same stationary depot energy

$$\begin{aligned} v &= \pm v_0, \\ e &= e_0 = \rho_0/d, \\ v_0 &= \pm \sqrt{(q_c/\rho_0 - c/d)}. \end{aligned} \quad (15)$$

We note that the coordinate $q(t)$ is not necessarily a linear length coordinate but may instead be the angle coordinate of a rotor [6, 21]. The SET model may be applied to problems of animal mobility [16, 19, 20, 22–26] and as shown above, may be mapped to our model of a fuel cell.

3.3. Problems of efficiency of the conversion of chemical to electrical energy

We study now the efficiency, which is as usual defined as the relation of energy flow used for some purpose to the total imported energy flow. For simplicity, we concentrate on energy conversion in the inner circuits following in large [9]. In a generalized mode, we do not fix here the number of operating circuits, assuming only that all have the same parameters, and consider \mathbf{J} and \mathbf{Q} as vectors:

$$\mathbf{Q} = [q_1, q_2, \dots, q_n], \quad \mathbf{J} = [j_1, j_2, \dots, j_n]. \quad (16)$$

The dynamical equations are in vectorial form

$$\begin{aligned} \frac{d\mathbf{Q}}{dt} &= \mathbf{J}, \\ L \frac{d\mathbf{J}}{dt} &= -R\mathbf{J} - \frac{\mathbf{Q}}{C} + \mathbf{U}_0 + de\mathbf{J}, \\ \frac{de}{dt} &= q_e - ce - de\mathbf{J}^2. \end{aligned} \quad (17)$$



Assume the relation of stationarity

$$I_0^2 = \mathbf{J}_0^2 = j_1^2 + j_2^2 + \dots = q_e/R - c_e/d; \tag{18}$$

$$e_0 = \frac{R}{d}.$$

Note that the dynamical properties of this more general model will be analyzed in a subsequent work. Here we consider only the stationary state which is the same for any dimensionality. There are two situations of special interest:

1. The energy is used to overcome an additional external dissipation, an extra resistance, and is converted to heat (or possibly light).

2. The energy is used to do useful mechanical or electrical work, possibly by bringing a charge to a higher potential level or driving an electromotor.

The first case is much easier in mathematical respect. We model the external dissipation by some additional unsymmetrical resistor R_1 . The model assumption is that the resistor which simulates a load acts only on positive currents, but not on negative currents. Then the negative currents remain

unchanged, however the positively directed currents will go down by some amount $\mathbf{I}_1^2 < \mathbf{I}_0^2$ determined by

$$\mathbf{I}_1^2 = \frac{q_c}{R + R_1} - \frac{c}{d}. \tag{19}$$

The corresponding shifted currents are with different signs

$$\pm \sqrt{\frac{q_c}{R + R_1} - \frac{c}{d}}. \tag{20}$$

The additional loss to overcome by the positive currents is $R_1 I_1^2$. This way we find for the efficiency

$$\eta = \frac{R_1 \mathbf{I}_1^2}{q_c} = R_1 \left(\frac{1}{R + R_1} - \frac{d}{c} \right). \tag{21}$$

Figure 11 shows that the efficiency increases first with the load and reaches a maximum around $r_1 \sim \sim R$. For any set of parameters, the efficiency curve stops at some critical load, i.e. the system stops here to work.

Now we investigate the case of constant counter voltage modeling a load. This is the situation where it is more difficult to bring the charge to a higher potential level. This situation is physically quite simple

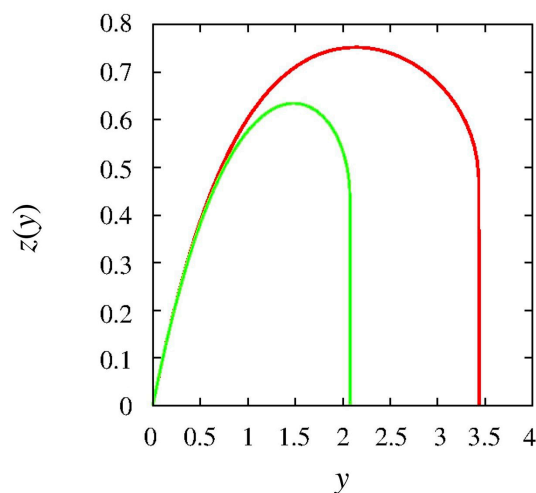
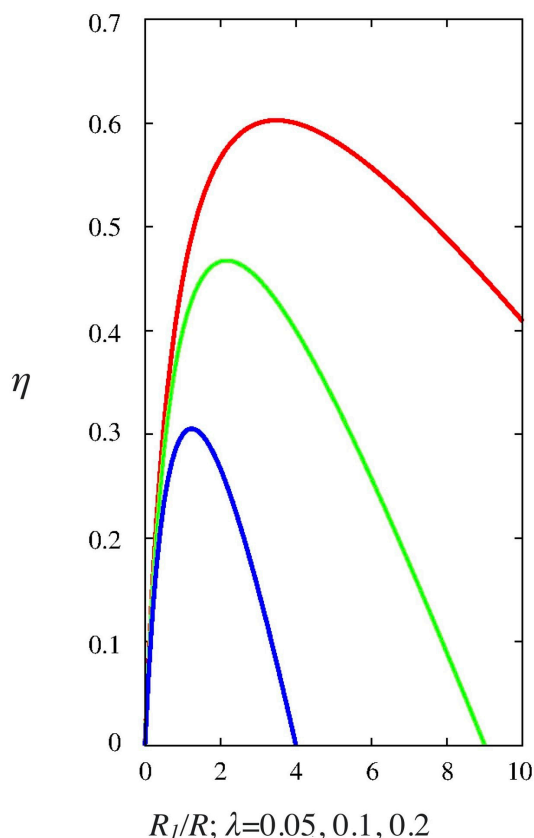


Fig. 11. Left panel: Efficiency of energy conversion η vs. dissipative load parameter with R_1/R for different parameters $\lambda = Rd = cq_c = 0.05, 0.1, 0.2$. Right panel: Efficiency z vs. a conservative load y for two quite low circuit loss parameters $\lambda = 0.05, 0.02$. We see again that for finite loss parameters, the curve stops at some critical load, corresponding to regions where Eq. (23) has no more real solutions, the regime where the circuit “works” breaks down (color online)



but mathematically more difficult. Without loss of generality, we assume that the additional voltage is directed to below $U_0 = -a$; $a > 0$, i.e. it tends to decrease the current. If a is small, the two attractors are shifted linearly in the force to lower values of the current

$$I_{01} = \pm I_0 - \frac{q_c a}{2R^2 I_0^2}; \quad E_1 = \frac{R}{d} \pm \frac{a}{I_0}. \quad (22)$$

For larger voltages, we have to solve nonlinear equations which we formulate in dimensionless variables:

$$y = \frac{a}{RI_0}; \quad \xi = \frac{I_1}{I_0}.$$

We find a cubic equation which is an implicit relation between current and load:

$$\xi^3 + y\xi^2 - \xi + \lambda y = 0; \quad \lambda = \frac{cR}{q_c d - cR}. \quad (23)$$

Here λ is a parameter describing the dissipation in the circuit and λy determines the character of the solutions. In the context of stochastic transitions, the case is of interest that the positive stationary currents approach each other and merge finally. The existence of real roots is bound to the condition that the discriminant of the cubic equation is positive $D(y, \lambda) > 0$. For $D(y, \lambda) < 0$ only downhill (i.e. less interesting) solutions exist. Looking for example at motor parameter $\lambda = 0.5$, the largest y which provides positive solutions for ξ is $y_{\max} = 0.28$. Our driven system is able to do work at the cost of chemical energy imported by the energy input $q_c > 0$. We define the thermodynamic efficiency as useful work against input of (chemical) energy into the depot

$$\eta = \frac{|U_0 I_1|}{q_c} = \frac{a I_1}{q_c}. \quad (24)$$

Here $I_1 = \xi_1 I_0$ is the stable “uphill” current corresponding to the largest positive root $\xi_1 > 0$. In some previous work [6,21], we used a linear approximation and found a parabolic dependence between efficiency and load with the maximum of efficiency

$$\eta_{\max} = \frac{1}{2}(1 - \lambda)^2, \quad (25)$$

which cannot exceed 50 percent reached for the case of no losses. Including nonlinear effects, we find using the dimensionless variables y, ξ for the efficiency $\eta = (1 + \lambda)\xi y$ the following equation for the variable $z = \xi y$

$$z^3 + y^2 z(z - 1) + \lambda y^4 = 0. \quad (26)$$

The solution expressing y in term of the efficiency variable z reads

$$y^2 = \frac{1}{2\lambda} z(1 - z) \pm \sqrt{\frac{1}{4\lambda^2} z^2(1 - z)^2 - \frac{1}{\lambda} z^3}. \quad (27)$$

The condition that the root in Eq. (27) should be real gives the largest possible value of efficiency

$$\eta_{\max} = (1 + \lambda) z_{\max}; \quad z_{\max} = 1 + 2\lambda - 2\sqrt{\lambda(1 + \lambda)}. \quad (28)$$

The optimal load is the value where the maximum is reached

$$y_{opt}^2 = \frac{1}{2\lambda} z_{\max}(1 - z_{\max}) = \frac{1}{\lambda^{1/2}} z_{\max}^{3/2}. \quad (29)$$

In the limit of small losses, the efficiency converges to 1 and the optimal load diverges as $\lambda^{-1/4}$. To give some examples, if $\lambda = 0.5$, the largest value of efficiency is $\eta_{\max} = 0.18$ and for $\lambda = 0.02$, we get the largest value $\eta_{\max} = 0.74$ at $y_{opt} = 2.1$. A graphical representation of the efficiency variable z against the load y is shown for $\lambda = 0.02$ and for $\lambda = 0.05$ in Fig. 11.

Analyzing Fig. 11 (right panel) shows that according to nonlinear effects the efficiency curve is not parabolic as the linear theory predicts [6, 21] but less symmetric and the maximum can be higher. It is interesting to note that in our case only nonlinear effects provide efficiencies better than 50 percent. For low losses and optimal load, the efficiency may approach one. However, for any finite quality parameter λ , the curve stops at some critical load, which corresponds to parameter regions where the cubic equation has no more real solutions. Then the uphill regime breaks down suddenly, not gradually. Only for the case of no losses $\lambda = 0$, the curve may reach for a special load the efficiency one. As the graphical solutions for the case of very low losses $\lambda = 0.05, 0.02$ clearly demonstrates, the efficiency may only for such low losses and optimal load reach values exceeding 60 or even 70 percent. In order to reach an efficiency of 100 percent, the internal losses in depot and motor must disappear $cR \rightarrow 0$. The model shows some interesting properties which qualitatively reproduce in particular the behavior against load which we expect from intuition and which was found already in other estimates and in experiments about molecular motors [22, 25–31]. In several simulations of the dynamical system, we observed for larger loads, say, $y > 1$ a low stability of the “hill-climbing state” in the numerical simulations. This means, that it might be quite difficult to realize the states with high efficiency. The influence of noise has



been studied based on the property that our dynamical system has a quasi-Hamiltonian character and a canonical distribution function [29].

4. More refined dynamical models and attractors of batteries

4.1. Time dependence and Nyquist plot

From the point of view of physics and nonlinear dynamics, batteries are highly nonlinear systems, as we have shown by means of attractors derived from measurements (see Figs. 5 and 7 in Sec. 1.1 and 1.2). The most characteristic time-dependent properties of battery cells to be explained by a dynamical model are reflected in the so-called Nyquist plot which is a standard tool of physics and electrical engineering. The Nyquist plot represents a plot of the real and imaginary parts of the impedance of a nonlinear electrical circuit. The most common use of Nyquist plots is for assessing the stability of a system with feedback. In Cartesian coordinates, the real part of the transfer function is plotted on the X axis and the imaginary part on the Y-axis (see, for example, Fig. 12). The Nyquist plot of Li-battery cells shows a quite typical shape. How useful this graphical method is for the investigation of stability of a given nonlinear system was first shown independently by the German electrical engineer Felix Strecker at Siemens in 1930 and the Swedish-American electrical engineer Harry Nyquist at Bell Telephone Laboratories in 1932. Nowadays called Nyquist criterion is a graphical technique for determining the stability of a dynamical system. Because it only looks at the Nyquist plot of the open loop

systems, it can be applied without making explicit the dynamical model of the system. Figure 12 shows the typical Nyquist plot empirically observed in investigations of Li-batteries. However, as found in many studies, the standard models based on usual differential equations of the type above, are unable to reproduce the frequency behavior reflected in the Nyquist plot. For this reason, more general dynamical models are needed [2]. In other words, one has to generalize the standard concept of circuits going to nonlinear noninteger order circuits which are more appropriate for describing the properties of batteries and fuel cells [2].

4.2. Dynamical models based on fractional calculus

In recent work, the idea came up to include fractional calculus for modeling the mechanism of nonlinear circuits including batteries and fuel cells [2, 14, 15, 32]. The processes in a lithium ion cell may be represented by a schema (Ersatzschaltbild) as proposed by Eckert [14] and by Wang et al. [15] (see Fig. 8). In mathematical terms, the model by Wang et al. [15] based on fractional calculus reads

$$D^{\alpha_1} x_1(t) = -\frac{x_1(t)}{R_1 C_1} + \frac{U(t)}{C_1}, \quad (30)$$

$$D^{\alpha_2} x_2(t) = -\frac{x_2(t)}{R_2 C_2} + \frac{U(t)}{C_2}, \quad (31)$$

$$D^1 x_3(t) = -\frac{\eta}{Q_n}. \quad (32)$$

We will try to map the dynamics of our system (Eqs. (2) and (3)) to a similar structure with the assumption of slowly changing currents $dI/dt = 0$ and

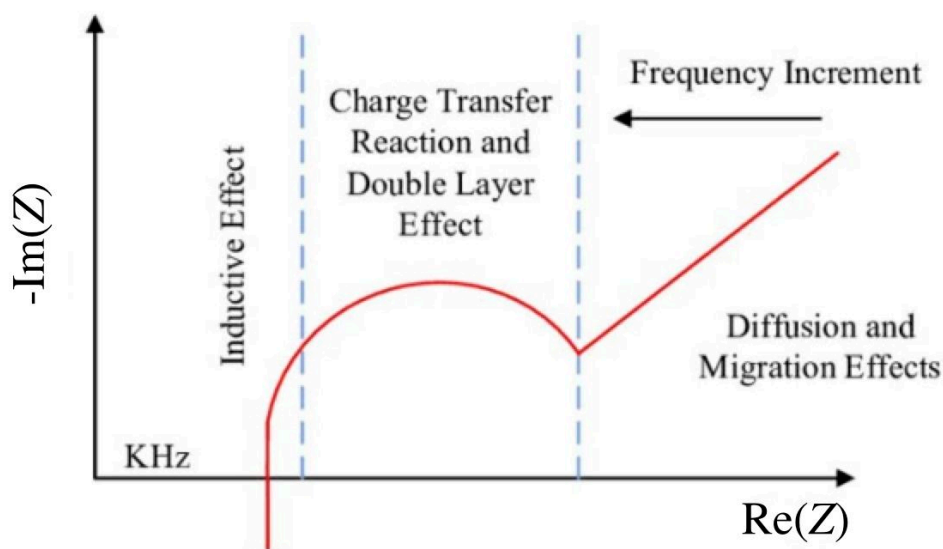


Fig. 12. Typical Nyquist plot of a Li-battery



time dependent input $q(t)$ and constant output U_0 , we get

$$\begin{aligned} \frac{dQ}{dt} &= I; \\ U_0 - R_0 I + U_e - V_c + deI &\cong 0; \\ \frac{de}{dt} &= q_e - ce - deI^2. \end{aligned} \quad (33)$$

Here is $V_c = Q/C$ the voltage at the capacitor. We study now the limit of slow current changes, what is equivalent to the assumption $L = 0$. This leads in the limit of slow current changes or $L = 0$ to the slow charge Q -dynamics. Further, we will use the assumption that the term U_e is small. Following the schema and notations proposed by Wang et al. and restricting to one circuit, we find for the voltage in that capacitor circuit and the current in the big circuit

$$\frac{dV_c}{dt} = \frac{I_0 - I}{C}, \quad (34)$$

$$\begin{aligned} 0 &= -R_0 I_0 - V_c + U_e + deI_0, \\ I_0 &\cong -\frac{V_c}{R_0} + \frac{V_0 + deI_0}{R_0}, \end{aligned} \quad (35)$$

$$\frac{de}{dt} = q_e - ce + de \frac{(V_c - U_e)^2}{(R + de)^2}.$$

These approximations lead us to a system of two differential equations:

$$\begin{aligned} \frac{dV_c}{dt} &= -\frac{V_c}{RC} + \frac{V_0 - V_c}{CR_0 + Cde}, \\ \frac{de}{dt} &= q_e - ce + de \frac{(V_0 - V_c)^2}{(R_0 + de)^2}. \end{aligned} \quad (36)$$

By introducing the dimensionless coordinates

$$\begin{aligned} y_1 &= V_c/V_{00}, \\ y_2 &= de/R_0, \\ \tau &= t/RC, \\ V_{00}^2 &= R_0^2/dR \end{aligned} \quad (37)$$

the two basic differential equations assume the form

$$\begin{aligned} \frac{dy_1}{d\tau} &= -y_1 + \frac{R}{R_0} \frac{(y_e - y_1)}{(1 + y_2)}, \\ \frac{dy_2}{d\tau} &= q_2 - y_2 \left[c_2 + \frac{(y_1 - y_e)^2}{(1 + y_2)^2} \right]. \end{aligned} \quad (38)$$

These two equations describe in our model the dynamics of the main battery variables y_1 standing for the internal voltage at the “capacitor” and y_2 standing for the battery charge, in dependence on the external load y_e . Positive load means, that the battery has to do work, negative load means that the battery is charged on the cost of the external voltage U_e . The internal voltage will increase, if $V_c > U_e$, i.e. $y_1 > y_e$ and otherwise it will decrease. The stationary state of this dynamical system of second order is defined by the two equations

$$\begin{aligned} (1 + y_2)^2 (c_2 y_2 - q_2) &= y_1 (y_1 - y_e)^2, \\ R_0 y_1 &= R (y_e - y_1) / (1 + y_2). \end{aligned} \quad (39)$$

The stationary point y_1^0, y_2^0 is located in the positive cone and small deviations $x_1 = y_1 - y_1^0, x_2 = y_2 - y_2^0$ satisfy linear equations. The stationary point is a circle of Lotka-Volterra type and the dynamics is Hamilton-like. A hypothetical generalization to fractional dynamics leads to two fractional differential equations for two dimensionless variables $y_1(\tau)$ and $y_2(\tau)$ and, similar as in the Wang model, however with different and more complicated r.h.s.

$$\begin{aligned} D^{\alpha_1} y_1(\tau) &= -\frac{y_1 - y_e}{1 + y_2}, \\ D^{\alpha_2} y_2(\tau) &= q_2 - y_2 \left[c_2 + \frac{(y_1 - y_e)^2}{(1 + y_2)^2} \right]. \end{aligned} \quad (40)$$

In addition, we have to include equations defining the battery input, which is here the chemical input $q(t)$ and the external battery load U_e . Needless to say that our model is beyond formal analogies, quite different from the models presented by Wang and by Eggert, and starts also from different physical assumptions. The justification of our model has to be checked of course in more detail. Possibly it may, however, allow to study problems connected with efficiency, which is in our extended model time-dependent and a function of $q(t)$ and U_e . Note that for studies of the stationary states and for efficiency in the stationary states, the transition from usual derivatives to fractal derivatives does not matter. The differences appear only in the time-dependent properties and in particular in the spectra.

Corresponding to the original background of the model, coming from fuel cell modeling, we may describe so far only one half of the processes in the battery, namely the half-cycle of discharging in a proper way; in this half cycle we should keep the chemical input $q(t)$ at zero or a very small value. The



other half-cycle, the loading (charging) process, we may approximate so far only by switching on the chemical input and keeping it on high level for a certain time in order to fill the chemical depot, then switching it off again, returning to the discharging cycle. The reverse cycle in which the model works backwards, which results by changing the sign of parameters, e.g. $d \rightarrow -d$ needs still further investigations.

5. Modeling battery networks, optimization and aging

5.1. Networking batteries and problems of optimization

There are many possibilities to connect batteries, however practically the simple parallel Kirchhoff networks are of main interest. In order to give an example for optimization of battery systems, let us consider a stochastic caricature of managing a battery system. We study a system of active elements (batteries) consisting of a constant number N of elements having in quantitative respect different properties measured by a number G_i and we consider a finite set of s different kinds of cells:

$$G_1, G_2, \dots, G_i, \dots, G_s \quad (41)$$

assuming that we have N_1 batteries in the class G_1 , N_i batteries of the class G_i etc. We start an optimization process like the evolutionary game studied by Manfred Eigen [33, 34]. We replace elements with the rate R_i and consider a destruction of elements with a rate D_i . By removing a bad element with a low valuation and replacing it by a copy of a good element in the set [33, 34], we come to an improvement of the functioning of the whole system. Instead of replacing, we may of course just recharge it. The dynamics of this process is such that all batteries which are better than the average, i.e.

$$G_i > \sum N_i G_i / \sum N_i \quad (42)$$

will increase their fraction x_i and all other will decrease it, what leads to the dynamics for the fractions $x_i = N_i/N$:

$$\begin{aligned} \dot{x}_i &= C(G_i - \langle G \rangle) x_i, \\ G_i &= R_i - D_i, \\ \langle G \rangle &= \sum G_i x_i. \end{aligned} \quad (43)$$

It may be shown easily that the average $\langle G \rangle$ increases, i.e. the system improves. This leads in the long run to an increasing average of quality of the whole system. The problem of replacing old or defect batteries in a battery system in an optimal way

may be solved by means of evolutionary algorithms [35–37]. The problem is related to the refueling of reactors. Strategies for solving the refueling problem have been developed in the 90ths for the optimization of power stations. Power stations are running by using certain fixed number of burning elements which have to be replaced for time to time by a fresh one [35]. This quite difficult problem may be successfully attacked by evolutionary algorithms. The problem of refueling or replacement of batteries in a network belongs mathematically to the same class and may be attacked therefore also by evolutionary algorithms.

5.2. Models including age as a dynamical variable

During a battery lifetime, its performance or “health” tends to deteriorate gradually due to irreversible physical and chemical changes that take place with usage (see Fig. 13). The physico-chemical reasons for aging are not yet fully explored. A study of Grolleau et al. [38] finds that the loss of lithium at the electrodes is the main aging mechanism [38]. Here we discuss only the question how to model aging processes. To ensure accurate State-of-Charge (SoC) calculation while a battery ages, the changes that take place in a battery over potential and Electro-Motive Force (EMF) behavior need to be fully understood [1].

Aging is a new concept in the theory of dynamical systems, which needs to introduce a new variable $\tau = t - t_0$, the internal time or lifetime. The notation gives already a hint to the close relation to living systems. In standard dynamical models, we have only one time as a variable and we study systems of differential equations for the set of variables $x_i(t)$. However, the dynamical systems to be studied here have an external time and a life time since they are aging.

In Sec. 1, we demonstrated on the example of experiments, how repeated charging and un-charging lead in combination with aging processes to quite typical changes in the time-dependence of voltage, current and other parameters including efficiency.

Figure 14 shows a simulation of a charging, un-charging process, i.e. periodic changes between a normal and a low input, accompanied by a slow aging of the battery. The aging process we simulated in the calculations is based on our battery model by a slow linear increase of internal damping $c_e(t) = c_e(0) + 0.00001t$ of the battery.

For systems having a life cycle, an additional variable τ plays a role, where $\tau > 0$ is the age between birth at $\tau = 0$ and death at some finite value of τ . In

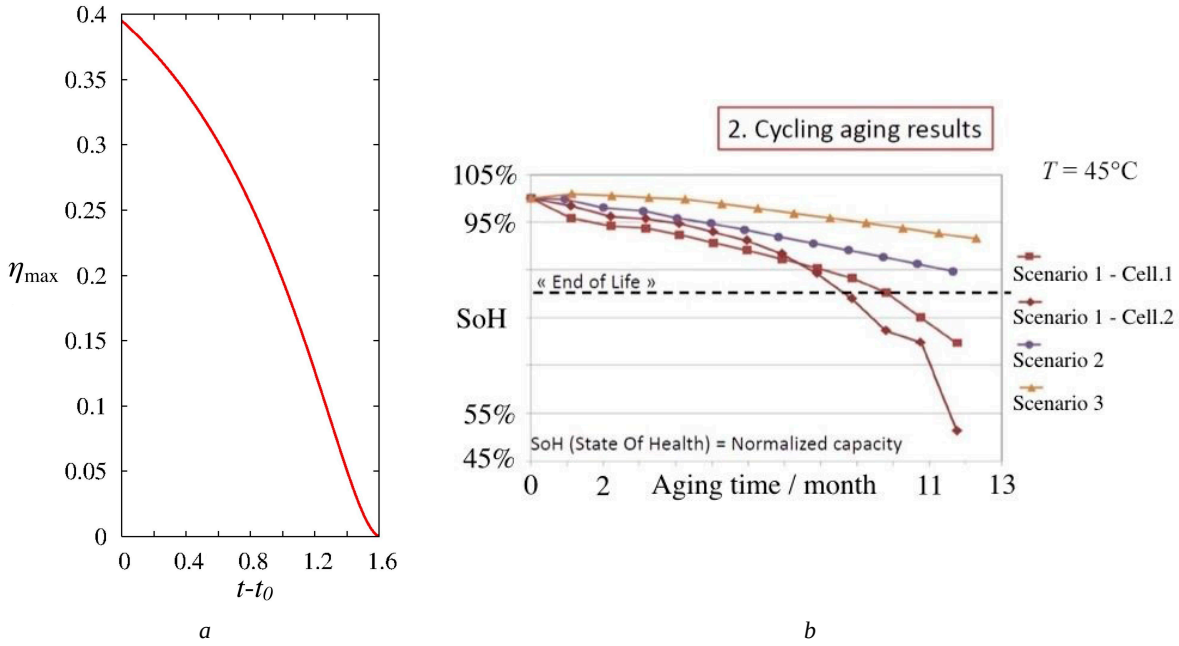


Fig. 13. Typical aging curves: (a) Decay of the efficiency due to increase of internal loss according to the present theory; (b) Empirical results about cycling aging [38]

the simplest case, only the parameters of the batteries depend on time, e.g.

$$\begin{aligned} L(\tau) \frac{dI}{dt} &= -R_0 I + U_e - V_c + d(\tau) eI, \\ \frac{de}{dt} &= q_e - c(\tau) e - d(\tau) eI^2. \end{aligned} \quad (44)$$

In our problem, birth means that a battery is inserted into the system and death means that a battery is removed from the system. In the simulation shown in Fig. 14, we assumed specific (given) regimes for the τ -dependence. Within our model of efficiency, we may assume e.g. that the internal losses increase in time linear or exponential in time

$$c_e(t) = c_0(1 + (\tau/\tau_1)), c_e(t) = c_0 \exp(\tau/\tau_1). \quad (45)$$

For the second example, Fig. 13(a) shows how the efficiency decreases within the lifetime of the battery; in Fig. 13(b) we show an empirically found loss off the voltage of a battery. In simplest case, we may stay within the old system of differential equations and consider only the parameters as depending on internal time. This is an approximation and Fig. 13(a) has been obtained this way. In a more complete theory, a life time-dependence leads to partial differential equations, as is well known from the theory of aging of living systems [33, 39, 40]. In the simplest case, we may model such a

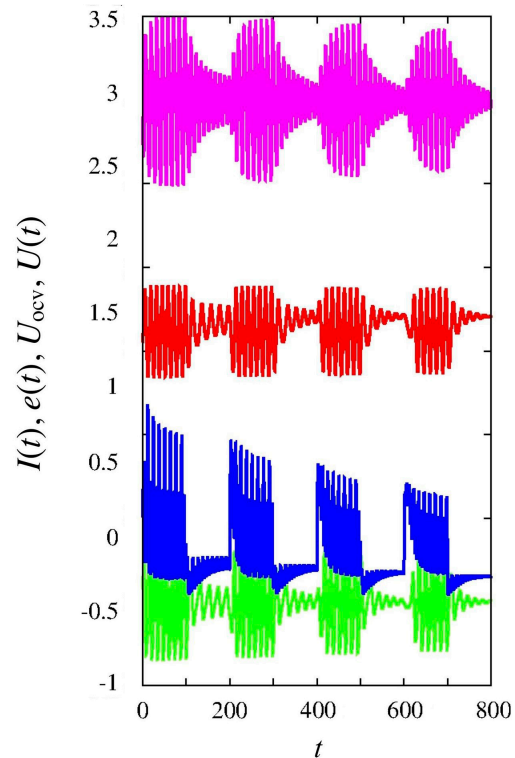


Fig. 14. Simulation of typical battery regimes including aging by means of our battery model. We assume a periodic change between the input $q_e = 0.8$ to $q_e = 0.2$ and vice versa and a small linear increase of the internal losses. We show (from below), the internal current in the circuit (below – green), the chemical energy in the depot (blue), the Open Circle Voltage (red), the total voltage (above – violet) for the time $t = 0-800$ assuming changes of the input strength q_e at $t = 100, 200, 300, 400, 500, 600, 700$ (color online)



system with the partial differential equations of so-called McKendrick–Von Foerster type [33, 39]:

$$\partial_t x_i(t, \tau) + \partial_\tau x_i(t, \tau) = -d_i(\tau) x_i(t, \tau), \quad (46)$$

$$\begin{aligned} x_i(t, 0) &= \int_0^\infty d\tau b_i(\tau) x_i(t, \tau), \\ x_i(0, \tau) &= \varphi_i(\tau), \quad i = 1, 2, \dots, n. \end{aligned} \quad (47)$$

Here $d_i(\tau)$ is the death rate of a battery depending on age, which is a characteristic function of batteries, further $b_i(\tau)$ is the birth rate. Note that we do not have own results based on the applications of McKendrick–Von Foerster type of equations to battery aging, we just wanted to point out here the appropriate mathematical tools.

Conclusion

Analysis of examples shows, without claiming for any completeness:

1. The conversion of chemical to electrical energy by isothermal processes is evidently not subject to “fundamental” upper bounds, like the Carnot upper bounds for the conversion of thermal to higher energy forms. As we have shown by two examples, efficiencies higher than 50 percent need as a rule the exploitation of nonlinear effects and a complete qualitative analysis of the properties for the nonlinear dynamical system.

2. The problem of optimization of efficiencies is connected with nonlinear dynamical systems with many system parameters. For such a dynamical multi-parameter problem, the purely empirical search based on “trial and error” is like a “search in the fog” and is at the end not a promising strategy. This leads to the request for more advanced search strategies and in particular for strategies which may be formulated and investigated analytically [35,36].

3. About load and efficiency: We analyzed simple models (macro models) of electrical circuits with three dynamical variables modeling the conversion of chemical into useful electrical energy. Sometimes models allow an analytical solution which may be used in particular for optimization. Some models show interesting properties which qualitatively reproduce in particular the decay with increasing load, which we expect intuitively and which was found also in several experiments [24]. Typically, the efficiency increases with the load and reaches a maximum near to an optimal load. High values above 50 percent may be reached only around optimal load and including the effect of special nonlinearities.

4. About aging and networking: Aging is a typical property of batteries, which may be modeled in

several ways. As an optimal choice of parameters for the elements and for networking it is recommended to find by stochastic evolutionary strategies [36].

Note added in May 2022: Correcting again and polishing this working paper written in first draft in 2019, the present authors feel obliged to follow and to complete the ideas suggested by our unforgettable friends and colleagues Vadim Anishchenko and Lutz Schimansky-Geier, who passed away within one and a half year after our meeting in Rostock not directly from, but within the turbulent times of the pandemy COVID19. We will never forget these unique personalities, gifted teachers, full of temperament and passion for nonlinear dynamics. We feel, it is our duty to go further the path, these great scientists paved into the wood of nonlinear stochastic processes in complex dynamical systems, like batteries and fuel cells as dynamical systems playing a central role in modern time.

References

- Hass E.-C., Knicker K., Sydow U., Schulz M., Plath P.-J. Battery – determination and forecast via Synergetics. In: Müller S. C., Plath P. J., Radons G., Fuchs A., eds. *Complexity and Synergetics*. Springer International Publishing AG, 2018, pp. 139–153. https://doi.org/10.1007/978-3-319-64334-2_12
- Arena P., Caponetto R., Fortuna L., Porto D. *Nonlinear Noninteger Order Circuits and Systems – An Introduction*. World Scientific, Singapore, 2000. 212 p. <https://doi.org/10.1142/4507>
- Anishchenko V. S., Astakhov V., Vadivasova T., Neiman A., Schimansky-Geier L. *Nonlinear Dynamics of Chaotic and Stochastic Systems*. Springer, 2007. 449 p. <https://doi.org/10.1007/978-3-540-38168-6>
- Newman J. S. *Electrochemical Systems*. 2nd edition. Englewood Cliffs, Prentice Hall, NJ, 1991. 560 p.; Newman J. S., Thomas-Alyea K. E. *Electrochemical Systems*. 3rd edition. Englewood Cliffs, Prentice Hall, NJ, 2004. 648 p.
- Chaturvedi N., Klein R., Christensen J., Ahmed J., Kojic A. Algorithms for advanced battery management systems. *IEEE Control Systems Magazine*, 2010, vol. 30, no. 3, pp. 49–68. <https://doi.org/10.1109/MCS.2010.936293>
- Romanczuk P. Bär M., Ebeling W., Lindner B., Schimansky-Geier L. Active Brownian Particles. From Individual to Collective Stochastic Dynamics. *Eur. Phys. J. Special Topics*, 2012, vol. 202, no. 1, pp. 1–162. <https://doi.org/10.1140/epjst/e2012-01529-y>
- Bachmann J. E. *Fuel Cells*. <https://wiki.uiowa.edu/display/greenergy/Fuel+Cells>
- Rychcik M., Skyllas-Kazacos M. Characteristics of a new all-vanadium redox flow battery, *J. of Power Sources*, 1988, vol. 22, iss. 1, pp. 59–67. [https://doi.org/10.1016/0378-7753\(88\)80005-3](https://doi.org/10.1016/0378-7753(88)80005-3)



9. Ebeling W., Feistel R. Energy conversion in isothermal nonlinear irreversible processes – struggling for higher efficiency. *Eur. Phys. J. Special Topics*, 2017, vol. 226, no. 9, pp. 2015–2030. <https://doi.org/10.1140/epjst/e2017-70014-2>
10. Joeriseen L., Garche J., Fabjan Ch., Tamozic G. Possible use of vanadium redox-flow batteries for energy storage in small grids and stand-alone photovoltaic systems. *J. of Power Sources*, 2004, vol. 127, iss. 1, pp. 98–104. <https://doi.org/10.1016/j.jpowsour.2003.09.066>
11. Gupta S., Lim T. M., Mushrif S. H. Insights into the solvation of vanadium ions in the vanadium redox flow battery electrolyte using molecular dynamics and metadynamics. *Electrochimica Acta*, 2018, vol. 270, pp. 471–479. <https://doi.org/10.1016/j.electacta.2018.03.008>
12. Afif A., Radenahmad N., Cheok Q., Shams S., Kim J. H. Ammonia-fed fuel cells: A comprehensive review. *Renewable and Sustainable Energy Reviews*, 2016, vol. 60, iss. C, pp. 822–835. <https://doi.org/10.1016/j.rser.2016.01.120>
13. Wang S., Fernandez C., Chunmei Y., Yongcun F., Wen C., Stroe D.-I., Chen Z. *Battery System Modeling*. Elsevier, 2021. 347 p. <https://doi.org/10.1016/C2020-0-03232-9>
14. Eckert M. *Modellbasierte Identifikation fraktionaler Systeme und Ihre Anwendung auf die Lithium-Ionen-Zelle*. KIT Scientific Publishing, Karlsruhe, 2017. 258 S. <https://doi.org/10.5445/KSP/1000071542>
15. Wang B., Liu Z., Li S. E., Moura S. J., Peng H. State-of-Charge estimation for Lithium-Ion batteries based on a nonlinear fractional model. *IEEE Transactions on Control Systems Technology*, 2017, vol. 25, iss. 1, pp. 3–11. <https://doi.org/10.1109/TCST.2016.2557221>
16. Ebeling W., Schweitzer F., Tilch B. Active Brownian motion with energy depots modeling animal mobility. *Biosystems*, 1999, vol. 49, no. 1, pp. 17–29. [https://doi.org/10.1016/S0303-2647\(98\)00027-6](https://doi.org/10.1016/S0303-2647(98)00027-6)
17. Tilch B., Schweitzer F., Ebeling W. Directed motion of Brownian particles with internal energy depot. *Physica A*, 1999, vol. 273, iss. 3–4, pp. 293–314. [https://doi.org/10.1016/S0378-4371\(99\)00247-2](https://doi.org/10.1016/S0378-4371(99)00247-2)
18. Li D., Sun Y., Yang Z., Gu L., Chen Y., Zhou H. Electrochemical oscillation in Li-ion batteries. *Joule (Cell Press)*, 2018, vol. 2, pp. 1265–1277. <https://doi.org/10.1016/j.joule.2018.03.014>
19. Schweitzer P., Ebeling W., Tilch B. Complex Motion of Brownian Particles with Energy Depots. *Phys. Rev. Lett.*, 1998, vol. 80, pp. 5044. <https://doi.org/10.1103/PhysRevLett.80.5044>
20. Erdmann U., Ebeling W., Schimansky-Geier L., Schweitzer F. Brownian particles far from equilibrium. *Eur. Phys. J. B*, 2000, vol. 15, pp. 105–113. <https://doi.org/10.1007/s100510051104>
21. Romanovsky Yu. M., Kargovsky A., Ebeling W. Models of Active Brownian Motors Based on Internal Oscillations. *Eur. Phys. J. Special Topics*, 2013, vol. 222, pp. 2465–2479. <https://doi.org/10.1140/epjst/e2013-02030-y>
22. Kolomeisky A. B., Fisher M. E. Molecular Motors: A Theorist's Perspective. *Annual Rev. of Phys. Chem.*, 2007, vol. 58, pp. 675–695. <https://doi.org/10.1146/annurev.physchem.58.032806.104532>
23. Ebeling W., Gudowska-Nowak E., Fiasaconaro A. Statistical distribution for Hamiltonian systems coupled to energy reservoirs and applications to molecular energy conversion. *Acta Phys. Pol. B*, 2008, vol. 39, no. 5, pp. 1251–1272.
24. Toyabe S., Muneyuki E. Experimental thermodynamics of single molecular motor. *Biophysics*, 2013, vol. 9, pp. 91–98. <https://doi.org/10.2142/biophysics.9.91>
25. Nishiyama M., Higuchi H., Yanagida T. Chemomechanical coupling of the forward and backward steps of single kinesin molecules. *Nature Cell Biol.*, 2002, vol. 4, pp. 790–797. <https://doi.org/10.1038/ncb857>
26. Harada T. Phenomenological energetics for molecular motors. *Europhys. Lett.*, 2005, vol. 70, no. 1, pp. 49–55. <https://doi.org/10.1209/epl/i2004-10456-2>
27. Richter P. H., Ross J. The efficiency of engines operating around a steady state at finite frequencies. *J. Chem. Phys.*, 1978, vol. 69, pp. 5521–5531. <https://doi.org/10.1063/1.436546>
28. Lipowsky R. Universal aspects of the chemomechanical coupling for molecular motors. *Phys. Rev. Lett.*, 2000, vol. 85, pp. 4401. <https://doi.org/10.1103/PhysRevLett.85.4401>
29. Feistel R., Ebeling W. *Physics of self-organization and evolution*. Wiley-VCH, Weinheim, 2011. 517 p. <https://doi.org/10.1002/9783527636792>
30. Schweitzer F. *Brownian agents and active particles*. Springer, 2003. 420 p. <https://doi.org/10.1007/978-3-540-73845-9>
31. Balmer R. T. *Modern Engineering Thermodynamics*. Academic Press, Elsevier, 2011. 827 p. <https://doi.org/10.1016/C2009-0-20199-1>
32. Barbosa R. S., Tenreiro Machado J. A., Vinagre B. M., Calderon A. J. Analysis of the van der Pol oscillator containing derivatives of fractional order. *J. of Vibration and Control*, 2007, vol. 13, iss. 9–10, pp. 1291–1301. <https://doi.org/10.1177/1077546307077463>
33. Ebeling W., Engel A., Feistel R. *Physik der Evolution-sprozesse*. Akademie-Verlag, Berlin, 1990. 371 S.
34. Ebeling W., Feistel R. Studies on Manfred Eigen's Model for the Self-Organization of Information processing. *Eur. Biophys. J.*, 2018, vol. 47, pp. 395–401. <https://doi.org/10.1007/s00249-018-1287-1>
35. Ebeling W., Schimansky-Geier L., Poeschel T., Aselmeyer T., Beule D., Buchholtz V., Erdmann U., Kappler C., Lieske R., Militzer B., Neiman A., Rose H., Rosenkranz D., Schautz F., Tilch B., Zamparelli M. *Evolutionary algorithms, EVOAL G. Foundations and applications of evolutionary algorithms*. Final report, BMBF 01IB403B. [https://hdl.handle.net/10068/153803\(1998\)](https://hdl.handle.net/10068/153803(1998))
36. Ebeling W., Rechenberg I., Schwefel H.-P., Voigt H.-M., eds. *Parallel Problem Solving from Nature*. PPSN IV, vol. 1141. Springer, 1996. 1076 p.



37. Bäck T., Heistermann T., Kappler C., Zamparelli M. *Evolutionary Algorithms Support Refueling of Pressurized Water Reactors*. Conference Paper, Research Gate, 1996. <https://doi.org/10.1109/ICEC.1996.542342>
38. Grolleau S., Delaille A., Gualous A. Lithium-ion battery aging. *27th Int. Electric Vehicle Symp.* Barcelona, 2013.
39. Romanovsky Yu. M., Stepanova N. V., Chernavsky D. *Mathematical Biophysics*. Moscow, Nauka Publ., 1984. 304 p. (in Russian).
40. Ebeling W., Engel A., Mazenko V. G. Modeling of selection processes with age-dependent birth and death rates. *Biosystems*, 1986, vol. 19, iss. 3, pp. 213–221. [https://doi.org/10.1016/0303-2647\(86\)90040-7](https://doi.org/10.1016/0303-2647(86)90040-7)

Поступила в редакцию 10.07.2022; одобрена после рецензирования 24.08.2022; принята к публикации 12.09.2022
The article was submitted 10.07.2022; approved after reviewing 24.08.2022; accepted for publication 12.09.2022